# A new approach to assess the effect of photodamage on corneocyte envelope maturity using combined hydrophobicity and mechanical fragility assays

D. Guneri* (iD), R. Voegeli† (iD), S. J. Gurgul*, M. R. Munday*, M. E. Lane* and A. V. Rawlings*

*UCL School of Pharmacy, 29-39 Brunswick Square, London WC1N 1AX, UK and †DSM Nutritional Products Ltd., PO Box 2676, Bldg. 205/315, Basel 4002, Switzerland

## Abstract

**BACKGROUND:** The maturity of the corneocyte envelope (CE) provides information about the barrier functionality of the stratum corneum (SC). Corneocytes are enclosed by the CE, a protein-lipid matrix, contributing to mechanical resistance and hydrophobicity of the SC.

**OBJECTIVES:** The aim of the work was to develop a novel and robust approach to characterize CE maturity based on rigidity, hydrophobicity and surface area. This offers an alternative approach to the Nile red staining and antigenicity of involucrin to characterize the CE. The photoexposed (PE) cheek and photoprotected (PP) post-auricular sites were selected for investigation.

**METHODS:** Nine tape strips were obtained from the cheek and post-auricular sites of healthy Caucasians. CEs on the first and last tape strip were subjected to sonication to assess rigidity, and Nile red staining to determine hydrophobicity per unit surface area. In addition, the presence of involucrin and lipids was assessed to determine CE maturity by examination of the red/green pixel ratio, percentage of involucrin expressing CEs and alternatively the ratio of fluorescence density.

**RESULTS:** The CE rigidity was lower in the deeper SC layers of the cheek, whereas post-auricular CEs were mechanically more resistant. Post-auricular CEs from the superficial SC had a larger surface area with a stronger fluorescence signal than those from the cheek. Interestingly, those CEs from the deeper SC layers had similar surface areas in both anatomical sites but were significantly different in hydrophobicity. These three parameters can be summarized as a relative CE maturity index that expresses CE maturity more precisely with a higher sensitivity than the conventional involucrin and Nile red staining approach. CEs of the cheek surface are more mature than CEs in the deeper SC layer, whereas CEs obtained from the post-auricular surface are more mature than those from the cheek surface.

**CONCLUSION:** The combined method developed allows characterization of CE maturity based on hydrophobicity per unit surface area and rigidity rather than a simple ratio of lipid to involucrin. A more robust and sensitive measurement has therefore been developed addressing the limitations of earlier protocols.

Correspondence: Dilek Guneri, UCL School of Pharmacy, 29-39 Brunswick Square, London, WC1N 1AX, UK. Tel.: +44 207 7535821; fax: +44 870 1659275; e-mail: d_gueneri@yahoo.de

## Résumé

**CONTEXTE:** la maturité de l'enveloppe cornée (EC) fournit des informations sur la fonction de barrière de la couche cornée (CC). Les cornéocytes sont entourés par l'EC, une matrice protéo-lipidique, qui contribue à la résistance mécanique et à l'hydrophobicité de la CC.

**OBJECTIFS:** l'objectif de ce travail était de développer une nouvelle approche robuste pour caractériser la maturité de l'EC d'après la rigidité, l'hydrophobicité et la surface. Il s'agit d'une approche alternative à la coloration au rouge de Nil et à l'antigénicité de l'involucrine pour caractériser l'EC. Des joues photoexposées (PE) et des sites post-auriculaires photoprotégés (PP) ont été sélectionnés pour l'étude.

**MÉTHODES:** neuf bandelettes ont été obtenues à partir de la joue et des sites post-auriculaires de personnes caucasiennes en bonne santé. Les EC de la première et de la dernière bandelette ont été soumises à une sonication afin d'évaluer la rigidité, et à une coloration au rouge de Nil pour déterminer l'hydrophobicité par unité de surface. De plus, la présence d'involucrine et de lipides a été évaluée afin de déterminer la maturité de l'EC en examinant le rapport de pixels rouge/vert, le pourcentage d'EC exprimant l'involucrine et de façon alternative le rapport de la densité de fluorescence.

**RÉSULTATS:** la rigidité de l'EC était inférieure dans les couches les plus profondes de la CC de la joue, alors que les EC post-auriculaires étaient mécaniquement plus résistantes. Les EC post-auriculaires provenant de la CC superficielle avaient une surface plus large avec un signal de fluorescence plus intense que celles provenant de la joue. Il est intéressant de noter que les EC des couches les plus profondes de la CC avaient des surfaces similaires dans les deux sites anatomiques, mais que leur hydrophobicité était sensiblement différente. Ces trois paramètres peuvent être résumés par un indice de maturité de l'EC relatif qui exprime la maturité de l'EC plus précisément avec une sensibilité plus élevée que l'approche utilisant l'involucrine et la coloration au rouge de Nil. Les EC de la surface de la joue sont plus matures que les EC situées dans la couche la plus profonde de la CC, alors que les EC obtenues à partir de la surface post-auriculaire sont plus matures que celles provenant de la surface de la joue.

**CONCLUSION:** la méthode combinée développée permet de caractériser la maturité de l'EC d'après l'hydrophobicité par unité de surface et la rigidité plutôt qu'un simple rapport de lipides sur

involucrine. Une mesure plus robuste et plus sensible a donc été développée pour répondre aux limites des protocoles précédents.

## Introduction

The skin has a unique homeostatic mechanism to maintain its integrity and barrier function. Epidermal stem cells in the basal layer differentiate into keratinocytes and migrate upwards towards the stratum corneum (SC) whereas changing dramatically in morphology and biochemistry. Keratinocytes become corneocytes when the cell nucleus and organelles have disintegrated, and lipid-filled lamellar bodies are released into the extracellular matrix [1]. In corneocytes, keratins are stabilized by disulphide bonds [2] and are aggregated with the aid of filaggrin [3] which drives the collapse of the 'ghost' cell into a flat polygonal shape [1]. Gradually, various structural proteins such as loricrin and involucrin are cross-linked by transglutaminases (TGases) to provide mechanical strength and replace the plasma cell membrane of keratinocytes with an insoluble corneocyte envelope (CE) [4]. Immature CEs mature with the covalent attachments of ceramides and fatty acids to involucrin and loricrin, possibly being mediated by TGase1 creating a hydrophobic coating. Additionally, those bound lipids may stabilize and strengthen the mechanical resistance of the CEs [5].

Nomarski contrast microscopy of CEs from different depths of the SC allowed the identification of two populations of CEs. These were characterized as immature 'fragile' CEs ($CE_f$) in the deeper SC layers and mature 'rigid' CEs ($CE_r$) in the superficial SC layers [6]. This finding was further confirmed by mechanical micromanipulation experiments where a higher force was needed to collapse the CEs from the SC surface compared to those from the deeper SC layers [7]. A further difference could be identified via Nomarski contrast microscopy and a tetramethylrhodamine isothiocyanate (TRITC) staining which binds to proteins and peptides thereby allows a non-selective visualization of CEs. Interestingly, the mechanically stabile $CE_r$ has shown a higher TRITC fluorescence intensity than the $CE_f$ [7].

Sonication is an alternative approach to the micromanipulation method to investigate the mechanical resistance of the CE which was developed to identify fragile envelopes in loricrin and 12R-lipoxygenase knock-out mouse models [8, 9]. Sonic waves of vibration are created in an ultrasonic bath which transmits the ultrasonic energy through the water into the samples. This method challenges the mechanical resistance of the CEs by shear forces to determine their rigidity and helps to distinguish $CE_f$ and $CE_r$ in a population of corneocytes.

In most recent years, the standard technique for assessing CE maturity has been based on the image analysis of visualized CE-bound lipids via Nile red staining combined with an immunostaining for the CE structural protein, involucrin. In the original protocol, CE maturity was expressed as a percentage of involucrin positive (+) CEs [10], whereas later studies adapted the measurement of red and green pixels to generate a ratio [11, 12]. The immunostaining and image analysis approaches have a number of limitations. For example, variation in the involucrin expression in different skin conditions may change the results obtained for CE maturity dramatically [10, 13]. Also, studies are not quantitatively comparable between the different methods [10]. Moreover, immunostaining may have drawbacks arising from variations in protocols that might have an effect on the antibody binding capacity or CE morphology such as increased risk for dehydration during various incubation steps

[10–12]. However, both analytical methods are associated with high standard errors and coefficients of variation.

In this study, we investigated CE maturity in photoexposed (PE) cheek and photoprotected (PP) post-auricular sites in healthy Caucasians while introducing a new and robust approach based on CE rigidity, hydrophobicity and surface area to characterize relative CE maturity (RCEM). Sonication was applied to examine the mechanical resistance of CEs and to distinguish between $CE_f$ and $CE_r$ whereas the Nile red staining method was assessed as the red fluorescence signal per surface area of the CEs. This approach was compared to previously reported methodology. In addition, the SC integrity, cohesion and thickness were assessed to determine correlations between transepidermal water loss (TEWL), protein content and CE maturity.

## Materials and Methods

### Study design

The study protocol was approved by the UCL Research Committee and the NHS London-Bromley Research Committee (Reference: 16/LO/1672). Caucasian healthy subjects (Fitzpatrick skin phototype II/III) were recruited without a history of skin disease who signed informed consent prior to participation in the study. The volunteers are seven females and males each in age $30 \pm 4$ years, median age 28 years, and were informed not to use any skin creams for at least 15 days before the SC sampling. The acclimatized skin ($21 \pm 1°C$; $35 \pm 5\%$ relative humidity) of volunteers was gently cleaned and allowed to dry at room temperature before TEWL measurements and tape stripping.

### Tape stripping and determination of SC integrity, cohesion and thickness

Nine successive standard D-Squame® tapes (diameter: 2.2 cm; area: 3.8 cm$^2$) (CuDerm Corporation, Dallas, TX, USA) were collected from the same area from all subjects. The sample collection was performed from the PE cheek (3 cm beneath the outer edge of the eye) and the PP post-auricular site (close to the earlobe). The pressure device provided by CuDerm Cooperation was used to apply 225 g cm$^{-2}$ pressure for 5 s with intervals of $20 \pm 5$ s between each tape [14] whereas each tape was removed with a single movement. The samples were stored at $-80°C$ until CE isolation.

Transepidermal water loss was measured (Aquaflux AF102, Biox Systems Ltd. London, UK) at baseline and $30 \pm 5$ s after the third, sixth and ninth tape stripping. The amount of protein collected from the SC was measured for infrared absorption (%) at 850 nm using the SquameScan™ 850A (Heiland Electronics GmbH, Wetzler Germany) and calculated using Eq. (1) [15].

$$\text{Protein Concentration } (\mu g \text{ cm}^{-1}) = 1.366 \times \text{Absorbance} (\%) - 1.557 \tag{1}$$

The TEWL measurements at baseline and with disruption of the barrier by tape stripping plus the amount of collected protein give information about the SC integrity, cohesiveness and thickness. The removed amount of SC by weight has been shown to correlate directly with the inverse TEWL [16]. However, the cumulative protein amount has been demonstrated a likewise relationship to determine the theoretical SC protein amount that could have been collected as well as an estimated SC thickness [17].

### Isolation of CEs

Corneocyte envelope maturity was determined from the first and ninth tape strip which are referred to as PE1 and PE9 for the cheek samples and PP1 and PP9 for the post-auricular samples. Each tape was cut in half to allow the comparison of the two isolation methods and CE maturity protocols. Half of the tapes were extracted with 750 $\mu$L of dissociation buffer containing 100 mM Tris-HCl pH 8.0, 5 mM EDTA, 2% SDS and 20 mM DL-dithiothreitol (Sigma Aldrich, Dorset, UK). Tapes were immersed in the dissociation buffer at 75°C for 10 min, shaken for 3 min at 1000 rpm room temperature and centrifuged for 10 min at 5000 $g$. The extracted CEs were washed by repeating the procedure three times in dissociation buffer [12].

The CEs from the other half of the tape were isolated similarly to the procedure above but with less salt and DL-Dithiothreitol generating a more gentle dissociation buffer (20 mM Tris-HCl pH 8.0, 5 mM EDTA, 2% SDS and 10 mM DL-Dithiothreitol) and a washing buffer (20 mM Tris-HCl pH 8.0, 5 mM EDTA, 0.2% SDS and 10 mM DL-Dithiothreitol) [8]. However, CEs collected from both isolation protocols were suspended in $1\times$ PBS buffer (Thermo Fisher Scientific, Hertfordshire, UK) instead of SDS containing buffers to allow a clear fluorescence signal without artefacts in the imaging progress.

### Immunostaining for involucrin and Nile red staining for lipids

Isolated CEs obtained via the described extraction protocol [11] were placed onto polysine-coated microscope slides (VWR international Ltd, Leicestershire, UK) each with 5 $\mu$L of CE suspension; this was carried out three times for each sample. Primary monoclonal antibody (1:100; mouse anti-human involucrin Cy5, Cambridge Biosciences, Cambridge, UK) was incubated overnight in a humidified chamber at 4°C. The antibody solution was washed with PBS three times for 5 min before adding the secondary antibody (1:100; FITC-coupled rabbit anti-mouse IgG, H&L chain, ABCAM PLC, Cambridge, UK) for 1 h at room temperature (in the dark) [10]. Slides were washed with PBS (three times for 5 min) and mounted with 20 $\mu$g mL$^{-1}$ Nile red (Sigma Aldrich, Dorset, UK) in 75% glycerol solution.

### Assessing CE maturity based on rigidity and hydrophobicity per surface area

Extracted CEs collected from the milder isolation protocol were divided into 20 $\mu$L aliquots with one being exposed to sonication (44 kHz) for 10 min at 4°C (Grant Instruments Ltd., Cambridgeshire, UK). The sonication was performed similar to a previously described protocol where a CEs were sonicated (40 kHz) at different temperatures and exposure times. It was shown that 4°C seemed to be the best temperature for sonication of CEs in, hence this temperature was chosen [8]. However, preliminary experiments were performed to determine the ideal exposure time to be 10 min. Sonicated and control CEs (three samples of 5 $\mu$L) were placed on a polysine-coated microscope slides (VWR international Ltd, Leicestershire, UK) and mounted with 20 $\mu$g mL$^{-1}$ Nile red in 75% glycerol solution to stain the lipid coating on CEs.

### Image and data analysis

Nine images were taken in total for each CE sample for both maturity assessment protocols. The fluorescence images were taken at a 10× objective magnification and were analysed via Image J® version 1.51j8 (National Institutes of Health, Bethesda, MD, USA); however, the image analysis differs from the previous reports as discussed further below.

Images were taken separately of immunostaining for involucrin and the Nile red staining. These images were analysed with three different alternatives of image analysis. The percentage of involucrin (+) CEs were determined to characterize CE maturity in accordance with the original protocol [10]. The recent analysis is to generate a red/green ratio from the total red and green pixels content determined by measuring the Red-Green-Blue (RGB) channels. In addition, the average CE surface area was determined from the 8-bit converted images where a threshold was set where all CEs are visible without influencing their size. Watershed was applied to define CE borders, allowing the detection of CEs with a surface area of 300–2000 $\mu$m$^2$ [11, 12]. Another red/green ratio was created by measuring the integrated density (fluorescence intensity per surface area) instead of a simple RGB channel measurement.

The images for our novel method were taken to investigate three different CE parameters. CE rigidity was determined for CE$_f$ and CE$_r$ by counting non-sonicated and sonicated CEs according to their morphological appearance.

$$\text{CE Rigidity} (\%) = \frac{\text{sonicated CEs}}{\text{control CEs}} \times 100 \qquad (2)$$

The CE hydrophobicity (fluorescence density) and surface area CEs were measured from the non-sonicated CEs. Similar to the previous method, the images were converted into 8-bit, inversion was applied to increase resolution, thresholding and watershed were adjusted. Image J was set to determine a surface area of 300–2000 $\mu$m$^2$, integrated density (fluorescence/surface area), and saved in the (Region of Interest) ROI manager. Once the CEs are marked in the ROI manager, individual 'rigid' CEs are selected only to exclude bias from any artefacts, however, then this image was closed. The original fluorescence image was opened to measure the fluorescence intensity and the surface area of the marked CEs. Correlating the hydrophobicity per surface area to rigidity (decimal number) results in the relative CE maturity as shown in Eq. (2) and expressed in arbitrary unit (AU):

$$\text{Relative CE Maturity} = \text{Fluorescence Density}\left(\frac{\text{red pixels}}{\mu\text{m}^2}\right) \times Rigidity \qquad (3)$$

### Statistics

Microsoft Excel® (Version 2013) was used for data collection and determination of the mean ± SD and statistical analysis was performed using GraphPad Prism (Version 6). All data passed the D'Agostino & Pearson normality test hence the statistical differences were analysed via a one-way ANOVA followed by the Sidak–Holm post-hoc test. All data are shown as mean ± SD ($n = 14$) and statistical significance is represented as *$P \leq 0.05$, **$P \leq 0.01$ or ***$P \leq 0.001$, in addition coefficient of variation (CV %) was determined.

## Results

### The conventional and alternative approaches to determine CE maturity via antigenicity of involucrin and lipid staining

The visual comparison for the fluorescence intensity in the superficial SC layers indicated PP1 have more lipids than PE1 samples. A
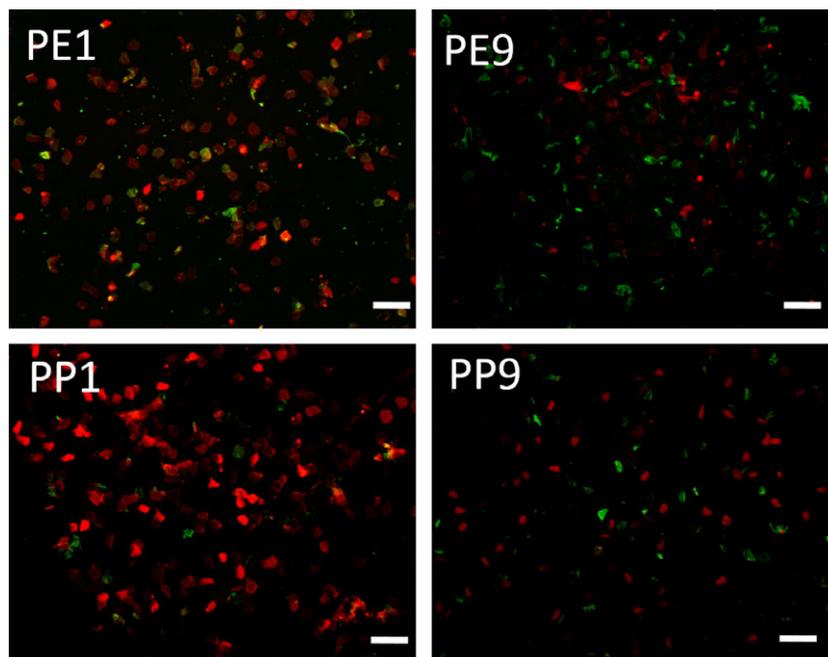
**Figure 1** Fluorescence images of PE cheek and PP post-auricular CEs from the superficial and deeper SC layers. Merged channels of green (involucrin) and red (lipids) fluorescence to visualize mature and immature CEs. PE1 = CEs of cheek, tape strip 1; PE9 = CEs of cheek, tape strip 9; PP1 = CEs of post-auricular, tape strip 1; PP9 = CEs of post-auricular, tape strip 9. Scale bar = 100 $\mu$m.
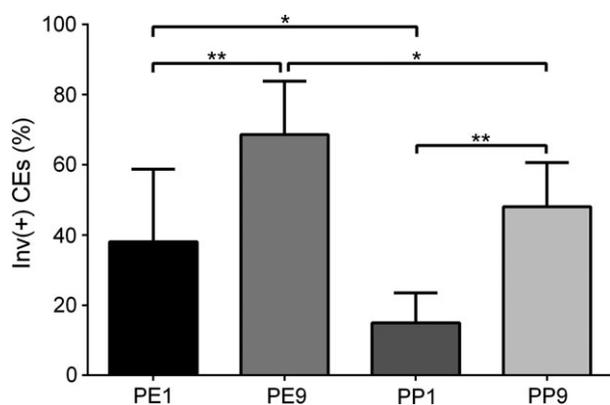


**Figure 2** Percentage of involucrin stained CEs. (n = 14; one-way ANOVA, post-hoc Sidak–Holm test; *p < 0.05 **p < 0.01, data are shown as mean±SD).
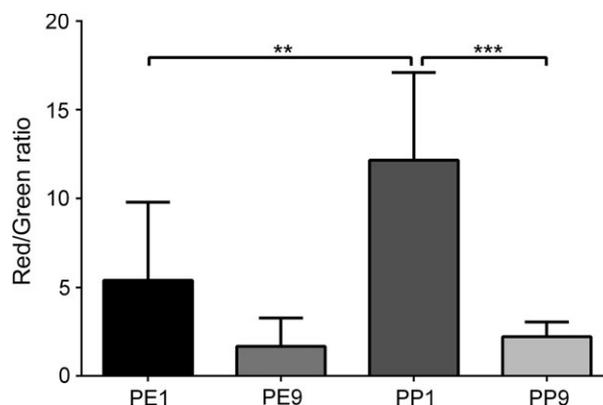


**Figure 3** Determination of CE maturity via red/green fluorescence. Image analysis for overall red and green channel to determine a ratio. (n = 14; one-way ANOVA, post-hoc Sidak–Holm test; **<p < 0.01; ***p < 0.001, data are shown as mean±SD).

higher population of immature CEs are located in the deeper SC layers compared to the superficial SC layers. There is a visual difference in fluorescence signal between PE9 and PP9 samples showing a relatively greater maturity in the PP samples (Fig. 1).

The percentage of immature CEs (Fig. 2) were determined from the obtained images of the involucrin and Nile red staining (Fig. 1). The SC surface of the PE cheek has 40.3 ± 21.8% (CV 54%) of immature CEs which rises to 67.7 ± 18.4% (CV 27.1%) of involucrin (+) CEs in the PE9 samples (P < 0.01). In the post-auricular SC surface, 15.8 ± 8.9% (CV 56.4%) of the CEs were stained for involucrin thereby less mature than PE1 (P < 0.05) as well as PP9 samples (P < 0.01). PP9 shows a similar CE maturity to the PE1 samples with 64.4 ± 22.8% (CV 35.5%) immature CEs, hence the PP9 samples are more mature than PE9 samples (P < 0.05).

Measurements of the red and green channel were used to determine the red/green ratio which corresponds to the CE maturity (Fig. 3) and confirmed that CEs from the superficial SC layers of both anatomical sites are more mature than those from the deeper SC layers. However, PP1 samples showed a significantly greater (P < 0.01) CE maturity ratio with 12.2 ± 4.9 (CV 40.6%) than 5.4 ± 4.4 (CV 81.4%) for PE1 samples. As indicated in the images (Fig. 1), PE9 are less mature with a ratio of 1.7 ± 1.6 (CV 97.3%) than those of PE1, however, the variation is too large to detect any statistical significance. CEs from the deeper SC of the post-auricular site are significantly (P < 0.001) less mature 2.2 ± 0.8 (CV 36.9%) than PP1 samples. The visual difference in CE populations between the deeper SC layers of both anatomical sites was not
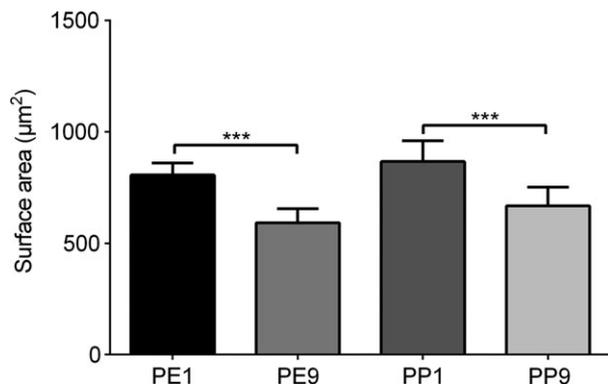
**Figure 4** Surface area of CEs in immunostaining approach. Images were analysed for their individual surface area values from the involucrin/Nile red staining. (n = 14; one-way ANOVA, post-hoc Sidak–Holm test; ***p < 0.001, data are shown as mean±SD).
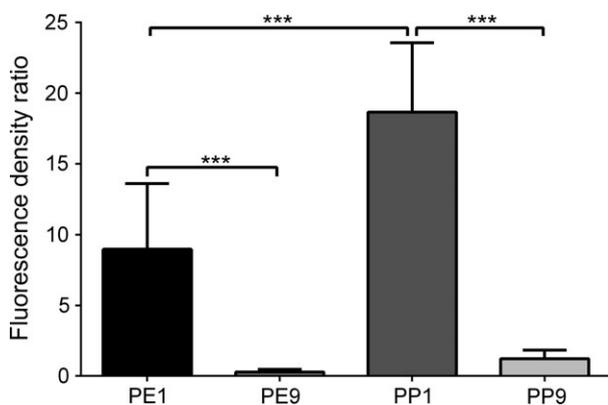


**Figure 5** Ratio of red and green fluorescence density. The CE maturity was determined on red and green pixels within individual CE surface area. (n = 14; one-way ANOVA, post-hoc Sidak–Holm test; ***p < 0.001, data are shown as mean±SD).

reflected via the image analysis of the red/green ratio determined via the RGB channel. Furthermore, the CE surface area was larger ($P < 0.001$) for CEs at the superficial layers compared to the deeper SC layers in both anatomical sides. No differences were found in CE surface area in the deeper SC layers of the PE cheek and PP post-auricular sites although those from the PE site were directionally smaller (Fig. 4).

An alternative image analysis was tested to generate the ratio of the red and green fluorescence intensity per individual CE surface area (Fig. 5) Using this approach, the fluorescence density ratio showed that PE1 is significantly more mature than PE9 ($P < 0.001$) and less mature then PP1 ($P < 0.001$). However, like the original red/green ratio method, PE9 showed no significant difference in the ratio of fluorescence density to that of PP9 which were still statistically less mature than CEs at the surface of the post-auricular SC ($P < 0.01$). This approach offered more sensitivity than the red/green ratio method but the discrimination between sites was still not clear as the percentage of involucrin (+) CE analysis.

### The 'new' approach to characterize CE rigidity, hydrophobicity and surface area

The fluorescence signal from Nile Red staining allows the visualization of the CE lipid coating and their morphology. CEs of PE1 have a higher fluorescence signal than PE9 but less than PP1 samples. Post-auricular CEs from the ninth tape strip have a distinctly higher fluorescence signal than PE9 but lower compared to CEs from the SC surface of the PP post-auricular site (Fig. 6).

The count of $CE_r$ and $CE_f$ gives the percentage of change in CE rigidity (Eq. (2)) showing that a 10 min sonication treatment allows a measurement of the resistance to mechanical stress in both anatomical sites and depths (Fig. 7). At the SC surface, the CEs have higher rigidity with 78.6 ± 8.7% (CV 11.1%) intact CEs in PE cheek and 85 ± 8.7% (CV 10.2%) in PP post-auricular CEs. The same vibration force revealed that only 43.4 ± 6.5% (CV 14.9%) CEs in the deeper SC layers of the PE cheek remain intact whereas 83.2 ± 8.9% (CV 10.7%) of CEs from PP9 were not affected by sonication ($P < 0.001$).

Corneocyte envelope hydrophobicity was evaluated by the fluorescence density for red pixels per surface area (Fig. 8) in the samples without sonication and confirmed the visual observations (Fig. 6). The PP post-auricular SC surface has CEs with a higher lipid content resulting in a fluorescence density of 28 392 ± 5218 red pixels $\mu m^{-2}$ (CV 18.4%) than the CEs in the PE cheek SC surface 16 331 ± 3341 red pixels $\mu m^{-2}$ (CV 20.5%) ($P < 0.001$). Also, CE hydrophobicity was significantly higher at the SC surface compared to the deeper SC layers in both anatomical sites ($P < 0.001$). Similar to the CEs at the surface of the PE cheek SC, the PE9 samples have a significantly lower fluorescence density ($P < 0.001$) with 9239 ± 1141 red pixels $\mu m^{-2}$ (CV 12.3%) than PP9 18 134 ± 3276 red pixels $\mu m^{-2}$ (CV 18.1%).

Surface area was determined for each individual CE from the first and ninth tape stripping of the PP post-auricular and PE cheek SC without sonication (Fig. 6). Post-auricular CEs from the SC surface are significantly larger with 1262 ± 96 $\mu m^2$ (CV 7.6%) than 1012 ± 116 $\mu m^2$ (CV 11.5%) from PE cheek SC surface ($P < 0.001$). Interestingly, the surface area of CEs from PE9 (836 ± 50 $\mu m^2$, CV 6%) was comparable to the values for PP9 (889 ± 106 $\mu m^2$, CV 12%) in the deeper SC layers (Fig. 9) but significantly different in hydrophobicity ($P < 0.001$) and rigidity ($P < 0.001$). Furthermore, the surface areas were larger compared with the red/green ratio and involucrin (+) CE analysis methods ($P < 0.001$).

These three parameters can be expressed as the RCEM by applying Eq. (3) which allows a comparison between the two anatomical sites and their surface and deeper SC (Fig. 10) with a higher sensitivity. Accordingly, PE cheek CEs are significantly more mature ($P < 0.001$) at the SC surface (12 735 ± 2420 AU, CV 19.1%) than at the deeper SC layers with 4015 ± 767 AU (CV 19.1%). CEs at the PP post-auricular surface are more mature with 24 214 ± 5796 AU (CV 23.9%) than 15 051 ± 2927 AU (CV 19.4%) in PE1 ($P < 0.001$) and PP9 ($P < 0.001$). The RCEM revealed that there is indeed a significant difference in CE maturity from the ninth tape strip of the PE cheek and PP post-auricular ($P < 0.001$). Although similar results were obtained compared with the involucrin (+) staining method, the CV's and statistical significance were considerably smaller ($P < 0.001$).
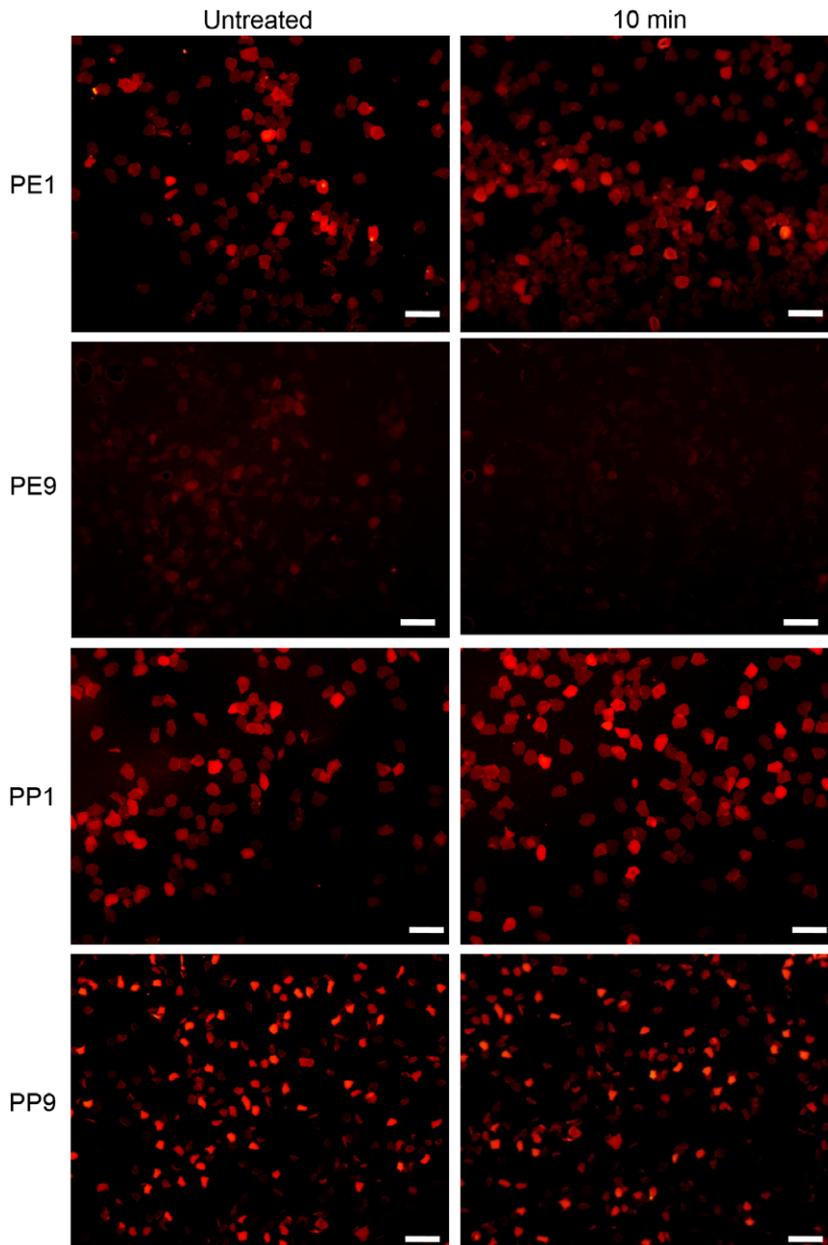
**Figure 6** Fluorescence images of CEs before and after 10 min of sonication in PE cheek and PP post-auricular. PE1 = CEs of cheek, tape strip 1; PE9 = CEs of cheek, tape strip 9; PP1 = CEs of post-auricular, tape strip 1; PP9 = CEs of post-auricular, tape strip 9. Scale bar=100 $\mu$m.

### SC integrity, cohesion and thickness in PE cheek and PP post-auricular

Transepidermal water loss and protein measurements were obtained at baseline and after the 3rd, 6th and 9th tape stripping to determine SC integrity and cohesion which was used to estimate SC thickness. PE cheek clearly showed a decreasing trend in protein levels, whereas the protein content in the PP post-auricular site remained constant throughout the tape strippings. This is reflected in the cumulative protein amount for the nine tape strips with $160 \pm 10$ $\mu$g cm$^{-2}$ (CV 6.25%) from the PP post-auricular SC but $132 \pm 11$ $\mu$g cm$^{-2}$ (CV 8.3%) of the PE cheek site ($P < 0.001$). A comparison of inverse TEWL values and cumulative protein amount was plotted to determine the maximum theoretical amount of SC protein that could have been collected (Fig. 11). Accordingly, PE cheek would have 195 $\mu$g cm$^{-2}$ and PP post-auricular site 555 $\mu$g cm$^{-2}$ SC protein which corresponds to an estimated SC thickness of 3.7 $\mu$m in PE cheek and 10.5 $\mu$m in PP post-auricular site. Nine tape strips removed $67.5 \pm 6\%$ (CV 8.9%) of the PE cheek but only $29.0 \pm 1.9\%$ (CV 6.5%) from the PP post-auricular site. Pearson's correlation coefficient ($r$) was analysed for the SC integrity as well as the cohesion and the CE maturity and the different approaches to determine CE maturity (Table 1). The CE maturity as determined by involucrin (+) CEs showed a positive
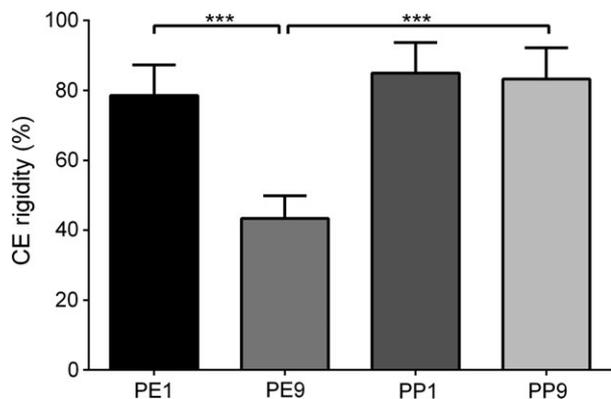
**Figure 7** CE Rigidity. Effect of sonication on CE rigidity in the SC layers. (n = 14; one-way ANOVA, post-hoc Sidak–Holm test; ***p < 0.001, data are shown as mean±SD).
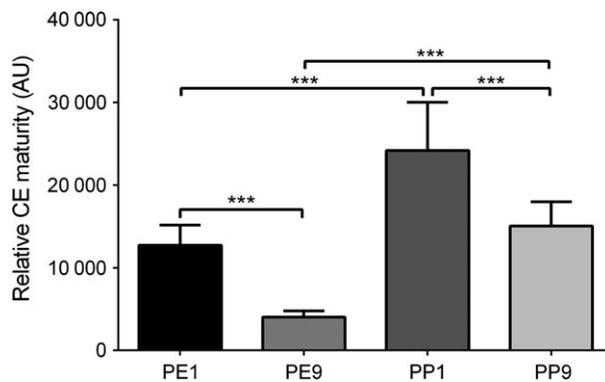


**Figure 8** CE Hydrophobicity. The fluorescence density was determined via the image analysis of non-sonicated CEs. This represents the lipid density in individual CEs of the PE cheek and PP post-auricular sites. (n = 14; one-way ANOVA, post-hoc Sidak–Holm test; ***p < 0.001, data are shown as mean±SD).



**Figure 9** CE Surface area. The surface area was determined for each CE isolated from the first and ninth tape of PE cheek and PP post-auricular sites. (n = 14; one-way ANOVA, post-hoc Sidak–Holm test; ***p < 0.001, data are shown as mean±SD).



**Figure 10** Relative CE maturity PE cheek and PP post-auricular sites from the first and ninth tape stripping. The RCEM determined from the hydrophobicity per CE surface area and rigidity shows the differences in CE maturity between anatomical sites and depth (n = 14; one-way ANOVA, post-hoc Sidak–Holm test; ***p < 0.001, data are shown as mean±SD).
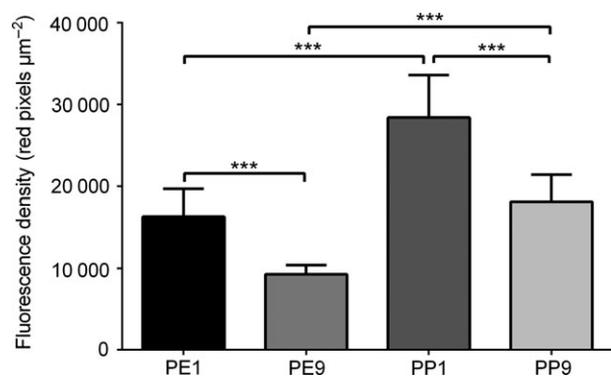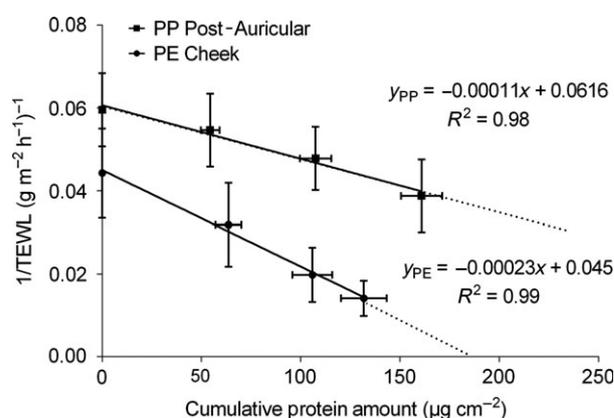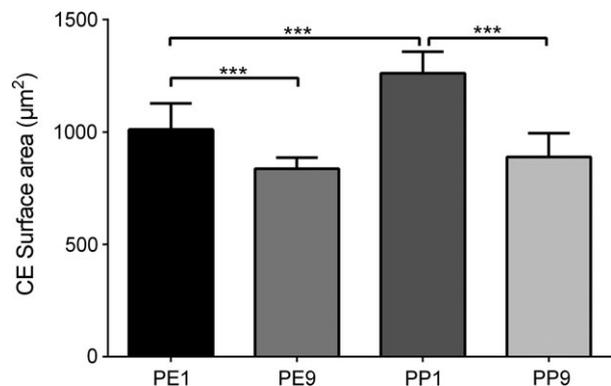


$$y_{PP} = -0.00011x + 0.0616$$
$$R^2 = 0.98$$

$$y_{PE} = -0.00023x + 0.045$$
$$R^2 = 0.99$$

**Figure 11** Determination of the theoretical SC thickness and integrity. The theoretical total amount of SC protein can be estimated at the x-intercept indicating that SC content for the PE Cheek is 195 $\mu$g cm-2 and the corresponding value for the PP Post-auricular site is 555 $\mu$g cm-2, consistent with a higher SC integrity and thickness in PP post-auricular site (n = 14, data are shown in mean±SD).

correlation in PE cheek ($r = 0.84$) and a negative correlation with the red/green ratio ($r = -0.74$), fluorescence density ratio ($r = -0.88$) and the RCEM technique ($r = -0.68$). In the PP post-auricular site, the CE maturity by involucrin (+) CEs ($r = 0.15$) and fluorescence density ratio ($r = 0.23$) showed no correlation. The current measurement for the red/green ratio showed a positive correlation ($r = 0.84$), whereas the RCEM demonstrated a negative correlation ($r = -0.76$) between SC integrity and CE maturity. The correlation of SC cohesiveness and CE maturity showed a negative correlation ($r = -0.88$) in PE cheek with a higher population of involucrin (+) CEs and positive correlation in red/green ratio ($r = 0.84$) and RCEM ($r = 0.91$) (Table 1). In the PP post-auricular, the RCEM demonstrated a positive correlation ($r = 0.96$) between increased SC protein collection and mature CEs whereas all others showed no correlation. This provides further confidence in the sensitivity of our novel approach especially for the CE characterization in the deeper SC layers of both anatomical sites.

**Table 1** Summary of Pearson's correlation coefficients between SC integrity and cohesion vs. CE maturity. The four methods of analysis were tested to determine CE maturity and the SC integrity in PE cheek and PP post-auricular sites.

| Pearson correlation coefficient | Inv (+) CEs | Red/Green ratio | Fluorescence density ratio | RCEM |
|---|---|---|---|---|
| PE Cheek SC integrity vs. CE maturity | 0.84 | −0.74 | −0.88 | −0.68 |
| PP Post-Auricular SC integrity vs. CE maturity | 0.15 | 0.84 | −0.23 | −0.76 |
| PE Cheek SC cohesiveness vs. CE maturity | −0.88 | 0.84 | −0.42 | 0.91 |
| PP Post-Auricular SC cohesiveness vs. CE maturity | −0.13 | 0.16 | 0.11 | 0.96 |

## Discussion

CE maturity analysis was originally based on morphology and TRITC staining [7], whereas Hirao and colleagues assessed CE maturity for the antigenicity for involucrin parallel to the Nile red staining for lipids [10]. The percentage of involucrin (+) CEs is indicative of CE immaturity in different skin conditions and ethnicities [10]. More recently, an image analysis-based method was developed to detect the overall red and green pixels for Nile red stained lipids and involucrin-FITC images to determine a ratio descriptive of corneocyte maturity. This approach has been applied to PE cheek and PP post-auricular CEs from the superficial (first tape) and deeper (ninth tape) SC layers of different ethnic groups to discriminate differences in CE maturity [18].

In the present study, the two conventional methods and a new method of evaluating CE hydrophobicity and mechanical integrity were compared for their accuracy and sensitivity. The previously reported red/green ratio approach showed a limitation in the discrimination of CE maturity in the deeper SC layers of both anatomical sites. Visual comparison shows a clear difference between PE9 and PP9; however, a ratio of the total red and green pixels of images from these sites failed to detect this difference. The post-auricular site has a higher protein content which might influence the involucrin staining hence influencing the ratio towards the immature CEs. The immunostaining for involucrin is a weakness of this method as its expression levels vary within a CE population and from the individual differences in participants [19, 20]. Moreover, the antibodies were reported to be applied in PBS [11, 12] instead of in the presence of a blocking solution as in the original protocol [10]. Depending on the antibody, this might not make a dramatic difference as shown by Buchwalow and colleagues [21]. The same primary and secondary antibodies were used as previous studies [11, 12] and evaluated in preliminary studies for the effect of blocking in the current project but no differences were evident.

The challenges of image analysis result in a wide range of values for the red/green ratios thus high standard errors and high CV's [11, 12, 22]. This is also the case when determining the percentage of involucrin (+) CEs [10, 13]. Moreover, comparing results between these two methods showed clear differences. Although the red/green ratio was capable of discriminating between photoexposed and non-photoexposed facial sites in tape 1 as reported previously [12], this method indicated no differences in CE maturity for the deeper samples. However, using the percentage of involucrin (+) CEs analysis approach does discriminate CE maturity at all SC depths. The red/green ratio per CE surface area did not show any significant differences in CE maturity in the lower layers of the SC again indicating reduced sensitivity of this approach.

The CE surface area has previously been reported to be 500–700 $\mu m^2$ for corneocytes sampled from the cheek surface SC, with no difference compared to the post-auricular site within the same ethnic group [18]. The involucrin/Nile red staining showed similar results (Fig. 4); however, our procedure demonstrated significant differences in the CE surface area from the superficial SC of PE cheek and PP post-auricular (Fig. 9).

Our new approach relies strongly on the surface area measurement and characterization of morphology of CEs in terms of their fragile-rigid appearance as well as their hydrophobicity and mechanical integrity and as a result the milder CE isolation protocol as described by Koch et al. was chosen [8]. The dissociation buffer with less salt and reducing agent and the washing buffer with lower detergent allowed a milder isolation process [8] compared with the harsher buffer of the original protocols [10] and, when resuspended in PBS, the samples had a reduced background fluorescence. In this present study, overall rigidity was assessed by counting CEs according to their morphological appearance with and without sonication. This mechanical stress revealed differences in the proportion of immature and fragile CEs especially in the deeper SC layers of the PE cheek site. Interestingly, PP post-auricular CEs seem to be less affected by mechanical stress for both the first and ninth tape strippings indicating differences in the mechanical stability probably mediated by crosslinking enzymes such as transglutaminases or differences in CE protein composition. A decrease in intact CEs was evident for the PE cheek CEs from the deeper SC with changes in values of $84.0 \pm 4.3\%$ at baseline to $36.4 \pm 5.4\%$ $(P < 0.001)$ after 10 min of sonication (data not shown) resulting in a CE rigidity of $43.4 \pm 6.5\%$ $(P < 0.001)$. CEs from the surface of the PE cheek and the both SC depths of the PP post-auricular were more resistant to sonication. Although mechanical behaviour of CEs from the volar forearm has been reported previously [7], the differences in facial CE rigidity with increasing depth into the SC using sonication as a mechanical challenge are reported here for the first time. This approach naturally offers advantages to the involucrin (+) and red/green ratio analyses as it precisely gives information of CE biomechanics and a true indicator of the mechanical fragility of the CE's that the other two methods do not. Indeed the PP9 samples would be reported as immature using conventional methodology but they are clearly not immature in their response to mechanical stress.

The second assay in our approach was to determine the hydrophobicity of the CE's per unit surface area rather than in relation to involucrin immunostaining. As variations were observed in sonicated CEs, showing a higher fluorescence signal which might result from rearrangement of lipids during the sonication process only non-sonicated CE's could be assessed. As expected, the hydrophobicity of facial CEs increases significantly towards the outer SC layers and as for the method of Hirao et al. [10, 13] discrimination between the different facial sites and depths was possible but subtle differences were observed for the relative maturity in CE's between the two methods.

Within a component of our RCEM calculation, we consider the SC barrier function is improved with increasing CE surface area which is supported by a previous study [23]. In our study, the surface area values of the CEs at the SC surface are indeed larger in both anatomical sites although the PP post-auricular CEs were larger than the PE cheek CEs indicating increased photodamage to the skin. However, the surface area of CEs from the ninth tape strip of both anatomical sites was comparable. Our new approach shows differences between the anatomical sites in the CE surface area in the superficial SC layers that were not detectable by the involucrin and Nile red staining.

Accordingly, we recommend that the RCEM should be determined according to the hydrophobicity of the CEs per unit surface area and rigidity as described in Eq. (3). The three parameters allow a more sensitive measurement of CE maturity than the conventional measurement of the red/green ratio and percentage of involucrin (+) CEs. The subtle depth differences in the PP site remain possibly due to similar mechanical characteristics of the CE's at the two depths but now even further discrimination is shown on the PE sites by our approach that considers the differences in hydrophobicity and the CE mechanical stability. As discussed previously, the red/green ratio method lacks the sensitivity to discriminate between CE's sampled from the deeper layers of the SC. Taking this new approach, the PP9 samples share similar CE hydrophobic and mechanical maturity properties to PE1 which is also reflected in the TEWL values.

All four methods showed a correlation between CE maturity and SC integrity in the PE cheek site. However, in the PP post-auricular site, there is a negative correlation with the RCEM for mature CEs and TEWL which reflects the increased SC integrity with CE maturity. The involucrin (+) CE, red/green ratio and RCEM showed a positive correlation between higher cumulative protein content and more mature CEs, indicating decreased SC cohesion with CE maturity. Interestingly, the RCEM is the only index amongst the approaches evaluated in this study that showed a positive correlation between CE maturity and SC cohesion. This is a further confirmation of the sensitivity of our novel approach especially for the CE characterization in the deeper SC layers of both anatomical sites.

Nevertheless, PE cheek corneocytes rigidify as they move towards the SC surface but they seem unable to gain increased hydrophobicity to the same extent as PP post-auricular corneocytes indicating UV-induced differences in SC enzymology between the studied facial sites. This is supported by the recent mass-spectrometric protein analysis of PE cheek and PP post-auricular SC [20]. As suggested by these studies, differences in the levels of 12R-lipoxygenase which primes the free omega-hydroxy ceramides for the transglutaminase-mediated hydrophobic enhancement of the CE's are lowered in photoexposed sites [20, 24]. Equally, reduced levels of loricrin may account for the increased fragility of the CE's [20].

In conclusion, as for previous studies, our findings suggest that the PP post-auricular SC is thicker and less compromised by tape strippings compared to the PE cheek [25]. However, for the first time, we demonstrated differences in CE rigidity between the PE cheek and PP post-auricular sites as well as differences in hydrophobicity. We propose the RCEM as a robust and sensitive assessment of CE maturity.

## Acknowledgements

## References

1. Candi, E., Schmidt, R. and Melino, G. The cornified envelope: a model of cell death in the skin. *Nat. Rev. Mol. Cell Biol.* **6**, 328–340 (2005).
2. Matoltsy, A.G. and Matoltsy, M.N. The chemical nature of keratohyalin granules of the epidermis. *J. Cell Biol.* **47**, 593–603 (1970).
3. Dale, B.A., Resing, K.A. and Lonsdale-Eccles, J.D. Filaggrin: a keratin filament associated protein. *Ann. N. Y. Acad. Sci.* **455**, 330–342 (1985).
4. Simon, M. and Green, H. Enzymatic cross-linking of involucrin and other proteins by keratinocyte particulates *in vitro*. *Cell* **40**, 677–683 (1985).
5. Nemes, Z., Marekov, L.N., Fesus, L. and Steinert, P.M. A novel function for transglutaminase 1: attachment of long-chain -hydroxyceramides to involucrin by ester bond formation. *Proc. Natl Acad. Sci.* **96**, 8402–8407 (1999).
6. Michel, S., Schmidt, R., Shroot, B. and Reichert, U. Morphological and biochemical characterization of the cornified envelopes from human epidermal keratinocytes of different origin. *J. Invest. Dermatol.* **91**, 11–15 (1988).
7. Harding, C.R., Long, S., Richardson, J., Rogers, J., Zhang, Z., Bush, A. and Rawlings, A.V. The cornified cell envelope: an important marker of stratum corneum maturation in healthy and dry skin. *Int. J. Cosmet. Sci.* **25**, 157–167 (2003).
8. Koch, P.J., de Viragh, P.A., Scharer, E. *et al.* Lessons from loricrin-deficient mice: compensatory mechanisms maintaining skin barrier function in the absence of a major cornified envelope protein. *J. Cell Biol.* **151**, 389–400 (2000).
9. Epp, N., Fürstenberger, G., Müller, K. *et al.* 12R-lipoxygenase deficiency disrupts epidermal barrier function. *J. Cell Biol.* **177**, 173–182 (2007).
10. Hirao, T., Denda, M. and Takahashi, M. Identification of immature cornified envelopes in the barrier-impaired epidermis by characterization of their hydrophobicity and antigenicities of the components. *Exp. Dermatol.* **10**, 35–44 (2001).
11. Mohammed, D., Matts, P.J., Hadgraft, J. and Lane, M.E. Depth profiling of stratum corneum biophysical and molecular properties: depth profiling of stratum corneum. *Br. J. Dermatol.* **164**, 957–965 (2011).
12. Raj, N., Voegeli, R., Rawlings, A.V., Gibbons, S., Munday, M.R., Summers, B. and Lane, M.E. Variation in stratum corneum protein content as a function of anatomical site and ethnic group. *Int. J. Cosmet. Sci.* **38**, 224–231 (2016).
13. Hirao, T., Takahashi, M., Kikuchi, K., Terui, T. and Tagami, H. A novel non-invasive evaluation method of cornified envelope maturation in the stratum corneum provides a new insight for skin care cosmetics. *Int. Fed. Soc. Cosmet. Chem. Mag.* **6**, 103–109 (2003).
14. Breternitz, M., Flach, M., Präßler, J., Elsner, P. and Fluhr, J.W. Acute barrier disruption by adhesive tapes is influenced by pressure, time and anatomical location: integrity and cohesion assessed by sequential tape stripping; a randomized, controlled study. *Br. J. Dermatol.* **156**, 231–240 (2007).

15. Voegeli, R., Heiland, J., Doppler, S., Rawlings, A.V. and Schreier, T. Efficient and simple quantification of stratum corneum proteins on tape strippings by infrared densitometry. *Skin Res. Technol.* **13**, 242–251 (2007).

16. Kalia, Y.N., Pirot, F. and Guy, R.H. Homogeneous transport in a heterogeneous membrane: water diffusion across human stratum corneum *in vivo. Biophys. J* . **71**, 2692–2700 (1996).

17. Mohammed, D., Yang, Q., Guy, R.H., Matts, P.J., Hadgraft, J. and Lane, M.E. Comparison of gravimetric and spectroscopic approaches to quantify stratum corneum removed by tape-stripping. *Eur. J. Pharm. Biopharm.* **82**, 171–174 (2012).

18. Raj, N., Voegeli, R., Rawlings, A.V., Summers, B., Munday, M.R. and Lane, M.E. Variation in the activities of late stage filaggrin processing enzymes, calpain-1 and bleomycin hydrolase, together with pyrrolidone carboxylic acid levels, corneocyte phenotypes and plasmin activities in non-sun-exposed and sun-exposed facial stratum cor. *Int. J. Cosmet. Sci.* **38**, 567–575 (2016).

19. Engelke, M., Jensen, J.M., Ekanayake-Mudiyanselage, S. and Proksch, E. Effects of xerosis and ageing on epidermal proliferation and differentiation. *Br. J. Dermatol.* **137**, 219–225 (1997).

20. Voegeli, R., Monneuse, J.-M., Schoop, R., Summers, B. and Rawlings, A.V. The effect of photodamage on the female Caucasian facial stratum corneum corneome using mass spectrometry-based proteomics. *Int. J. Cosmet. Sci.* **39**, 637–652 (2017).

21. Buchwalow, I., Samoilova, V., Boecker, W. and Tiemann, M. Non-specific binding of antibodies in immunohistochemistry: fallacies and facts. *Sci. Rep.* **1**, 28 (2011).

22. Mohammed, D., Matts, P.J., Hadgraft, J. and Lane, M.E. Variation of Stratum Corneum Biophysical and Molecular Properties with Anatomic Site. *AAPS J* **14**, 806–812 (2012).

23. Gorcea, M., Hadgraft, J., Moore, D.J. and Lane, M.E. *In vivo* barrier challenge and initial recovery in human facial skin. *Skin Res. Technol.* **19**, 375–382 (2013).

24. Muñoz-Garcia, A., Thomas, C.P., Keeney, D.S., Zheng, Y. and Brash, A.R. The importance of the lipoxygenase-hepoxilin pathway in the mammalian epidermal barrier. *Biochim. Biophys. Acta BBA - Mol. Cell Biol. Lipids* **1841**, 401–408 (2014).

25. Voegeli, R., Rawlings, A.V. and Summers, B. Facial skin pigmentation is not related to stratum corneum cohesion, basal transepidermal water loss, barrier integrity and barrier repair. *Int. J. Cosmet. Sci.* **37**, 241–252 (2015).